Title: BEN3/BIG2 ARF GEF is Involved in Brefeldin A-sensitive Trafficking at the *trans*-Golgi Network / Early Endosome in *Arabidopsis thaliana*

Running head: BEN3 ARF GEF in TGN to PM traffic

Corresponding author: Dr. H. Tanaka

Department of Biological Sciences, Graduate School of Science, Osaka University, 1-1 Machikaneyama-cho, Toyonaka-shi, Osaka 560-0043, Japan

Tel: +81-(0)6-6850-5984

E-mail: hirokazu.tanaka@bio.sci.osaka-u.ac.jp

Subject areas: (7) membrane and transport

This manuscript contains 1 black figure, 4 colour figures, 7 supplementary figures and 2 supplementary tables.

BEN3/BIG2 ARF GEF is Involved in Brefeldin A-sensitive Trafficking at the *trans*-Golgi Network / Early Endosome in *Arabidopsis thaliana*

Saeko Kitakura[1,2], Maciek Adamowski[3], Yuki Matsuura[1], Luca Santuari[5], Hirotaka Kouno[1], Kohei Arima[1], Christian S. Hardtke[5], Jiří Friml[3,4], Tatsuo Kakimoto[1], Hirokazu Tanaka[1*]

1. Department of Biological Science, Graduate School of Science, Osaka University, Osaka 560-0043, Japan
2. Present address: Graduate School of Agriculture, Kyoto University, Kyoto 606-8502, Japan
3. Institute of Science and Technology Austria (IST Austria), 3400 Klosterneuburg, Austria
4. Mendel Centre for Plant Genomics and Proteomics, Central European Institute of Technology (CEITEC), Masaryk University (MU), Kamenice 5, Brno, CZ-625 00 Czech Republic
5. Department of Plant Molecular Biology, University of Lausanne, Biophore Building, Lausanne CH-1015, Switzerland.

* Author for correspondence: hirokazu.tanaka@bio.sci.osaka-u.ac.jp

Abbreviations: ARF, ADP ribosylation factor; *ben3*, *bfa-visualized endocytic trafficking defective 3*; BFA, brefeldin A; EE, early endosome; GEF, guanine nucleotide exchange factor; PIN, PIN-FORMED; PM, plasma membrane; TGN, *trans*-Golgi network.

Total characters: 57,067. (8,386 words)

Abstract

Membrane traffic at the *trans*-Golgi network (TGN) is crucial for correctly distributing various membrane proteins to their destination. Polarly localized auxin efflux proteins, including PIN-FORMED1 (PIN1), are dynamically transported between the endosomes and the plasma membrane (PM) in the plant cells. The intracellular trafficking of PIN1 protein is sensitive to a fungal toxin brefeldin A (BFA), which is known to inhibit guanine-nucleotide exchange factors for ADP ribosylation factors (ARF GEFs) such as GNOM. However, the molecular details of the BFA-sensitive trafficking pathway have not been revealed fully. In a previous study, we have identified an Arabidopsis mutant *BFA-visualized endocytic trafficking defective 3* (*ben3*) which exhibited reduced sensitivity to BFA in terms of BFA-induced intracellular PIN1 agglomeration. Here, we show that *BEN3* encodes a member of BIG family ARF GEFs, BIG2. Fluorescent proteins tagged BEN3/BIG2 co-localized with markers for TGN / early endosome (EE). Inspection of conditionally induced de novo synthesized PIN1 confirmed that its secretion to the PM is BFA-sensitive and established BEN3/BIG2 as a crucial component of this BFA action at the level of TGN/EE. Furthermore, *ben3* mutation alleviated BFA-induced agglomeration of another TGN-localized ARF GEF BEN1/MIN7. Taken together our results suggest that BEN3/BIG2 is an ARF GEF component, which confers BFA sensitivity to the TGN/EE in Arabidopsis.

Key words: *trans*-Golgi network, brefeldin A, ARF GEF, auxin, PIN-FORMED1, Arabidopsis.

Introduction

Correct localization of proteins at the membrane systems is of crucial importance in eukaryotic organisms. In plants, various membrane proteins including transporters and receptor-like kinases localize to distinct plasma membrane domains and play key roles in transporting plant hormones and nutrients as well as intercellular signaling (Gälweiler et al., 1998; Müller et al., 1998; Friml et al., 2002a, 2002b; Swarup et al., 2001; Takano et al., 2002; Watanabe et al., 2004; Takano et al., 2010; Pfister et al., 2014; Takeuchi and Higashiyama, 2016). PIN family proteins are well-characterized auxin efflux transporters. In Arabidopsis, five PIN proteins, PIN1, 2, 3, 4, 7, which express in distinct and overlapping patterns, localize asymmetrically at the plasma membrane and collaboratively involved in polar auxin transport (Adamowski and Friml, 2015).

Localization studies have revealed that the polar localization of PIN proteins dynamically changes according to developmental signal during organogenesis (Benková et al., 2003) or embryogenesis (Friml et al., 2003) and tropic responses (Ding et al., 2011; Leitner et al., 2012; Rakusová et al., 2011, 2016). Pharmacological and genetic studies have demonstrated that these dynamic changes of PIN proteins as well as steady-state polar localization at the plasma membrane are achieved by the collective action of the membrane trafficking system (Geldner et al., 2001, 2003; Kleine-Vehn et al., 2008a). A chemical inhibitor brefeldin A (BFA) triggers a rapid agglomeration of endomembrane compartments and accumulation of membrane proteins including PIN1 in these compartments in Arabidopsis seedling roots (Geldner et al., 2001). These agglomerated endosomal compartments contain the *trans*-Golgi network (TGN) / early endosome (EE) accumulated at their core, and are called as ‘BFA bodies’ or ‘BFA compartments’. This rapid PIN1 relocation reveals constitutive endocytosis and BFA-sensitive exocytic PIN1 trafficking (Geldner et al., 2001, 2003; Kleine-Vehn et al., 2008a; Richter et al., 2014), which potentially allow dynamic redistribution of PIN1 in response to endogenous

developmental stimuli including different plant hormones (Benková et al., 2003; Paciorek et al., 2005; Marhavý et al., 2011; Löfke et al., 2013; Du et al., 2013).

Efficient PIN1 accumulation at the BFA compartment requires endocytosis, which depends on clathrin, dynamin-like protein, sterol methyltransferase SMT1 and GNOM-LIKE1 ARF GEF acting redundantly with GNOM (Richter et al., 2007; Teh and Moore, 2007; Men et al., 2008; Naramoto et al., 2010; Mravec et al., 2011; Kitakura et al., 2011) as well as a Sec1/Munc18 protein BEN2/VPS45 potentially involved in membrane fusion at the TGN/EE (Tanaka et al., 2013). In addition, BFA-sensitive GBF-type ARF GEF GNOM relocates from Golgi apparatus to the core of the BFA compartment in the presence of BFA and is necessary for accumulation of PIN1 at the BFA compartments (Geldner et al., 2003; Naramoto et al., 2014b). Other ARF GEFs BEN1/MIN7, BIG3 and BIG4, which belong to BIG subfamily, localize at the TGN/EE, and upon BFA treatment they localize at the core of the BFA compartments (Tanaka et al., 2009; Richter et al., 2014). BEN1/MIN7 is required for efficient agglomeration of PIN1 at the BFA compartment (Tanaka et al. 2009), whereas BIG3 and possibly its homologues are positively involved in secretory trafficking of PIN1 (Richter et al. 2014). In addition, exocytic trafficking from the TGN/EE appears to involve BEX1/ARF1A1C (Tanaka et al., 2014), interactor of constitutively active ROP/ROP interacting partner1 ICR1/RIP1 (Hazak et al., 2010), VAN4/TRS120 (Naramoto et al., 2014a), BEX5/RabA1b (Feraru et al., 2012), and exocyst components (Drdová et al., 2013). However, molecular mechanisms underlying BFA-sensitive PIN1 exocytic trafficking are not fully understood.

In the previous studies, we have carried out forward genetic screens for Arabidopsis mutants with altered PIN1-GFP distribution in BFA-treated seedling roots. Based on the BFA-responsive phenotypes, the identified mutants have been classified into either *ben* or *bex* mutants (Tanaka et al. 2009; Tanaka et al. 2014). Intracellular accumulation of PIN1-GFP in response to BFA

treatment was less pronounced in the *ben1* to *ben3* mutants (Tanaka et al. 2009), whereas it was exaggerated in *bex1* and *bex5* mutants (Feraru et al. 2012; Tanaka et al. 2014). Molecular cloning of the responsible genes identified BEN1 ARF GEF, BEN2/VPS45, BEX1/ARF1A1C, and BEX5/RabA1b, which are involved in trafficking at the TGN/EE. Here, we describe molecular cloning of the *BEN3* gene, whose mutation is responsible for the defective PIN1 trafficking observed in the *ben3* mutant. Our results show that *BEN3* encodes the BIG2 ARF GEF, localizes at the TGN/EE and is involved in TGN/EE to PM trafficking. Based on the BFA-insensitive PIN trafficking phenotypes of *ben3* and BFA-sensitive localization of fluorescently tagged BEN3/BIG2, and BEN3-dependent localization of BEN1/MIN7 at the BFA compartment, we propose that BEN3/BIG2 is a BFA sensitive ARF GEF functioning at the TGN/EE.

Results

Molecular cloning reveals that *ben3-1* has a non-sense mutation in the *ARF GEF BIG2* gene

In order to identify the mutation responsible for the *ben3* phenotype, *ben3-1; PIN1-GFP* line was subjected to whole genome sequencing. Analysis of the sequence data revealed that the *ben3-1* mutant contained nonsense mutations in two ORFs (Table S1). Among them, a mutation in the gene for BIG2 ARF GEF (At3g60860) was predicted to cause a premature stop codon (Supplementary Fig. S1A). GBF and BIG family ARF GEFs from eukaryotes share dimerization and cyclophilin binding (DCB), homology upstream of Sec7 (HUS), catalytic Sec7, homology downstream of Sec7 (HDS) domains (Mouratou et al., 2005). Likewise, Arabidopsis BIG2 contains DCB, HUS, Sec7, HDS1, HDS2, and HDS3 domains (Mouratou et al. 2005). In addition, comparison of the predicted amino acid sequences of BIG2 homologues revealed that C-terminal region was conserved among putative homologues of BIG2 in various plant species (Supplementary Fig. S1B). The site of *ben3-1* mutation corresponded to the C-terminal region. Together with rough mapping results (Tanaka et al. 2009), we reasoned that the mutation in the *BIG2* gene might be responsible for the *ben3* mutant phenotype. To test this possibility, we generated a *BIG2::BIG2-RFP* construct and transformed it into the *ben3-1* mutant. Whereas BFA-treated *ben3-1* mutant exhibited reduced PIN1-GFP agglomeration, *ben3-1* seedlings harboring the *BIG2-RFP* construct (hereafter called *ben3-1; BEN3-RFP*) exhibited clear agglomeration of PIN1-GFP as in wildtype (n=40, Supplementary Fig. S1C), indicating that the *BEN3-RFP* rescued the *ben3-1* mutant phenotype.

Multiple *big2* alleles are associated with BFA-sensitive PIN1 trafficking defects

To test whether the *BIG2* gene is involved in BFA-sensitive PIN1 trafficking, independently identified *big2* mutants were treated with BFA and immunostained with anti-PIN1 antibody. Sites of the T-DNA insertions in SALK_093944, SALK_016558, and SALK_024602 correspond to the DCB, HDS2 domains, or downstream of the HDS2 domain of BIG2 (Supplementary Fig. S1A). These T-DNA insertion *big2* mutants exhibited BFA-visualized PIN1 trafficking defects strongly resembling that in *ben3-1* (Fig. 1 A). These results suggested that the T-DNA insertions disrupted the *BIG2* gene, even though RT-PCR experiments revealed that partial *BIG2* transcripts are present in these T-DNA alleles (Supplementary Fig. S2A, B). We further generated a new *ben3* allele, *ben3-CRISPR*, harboring a frame-shift mutation in the 4th exon of the *BIG2* gene by using CRISPR-Cas9 system to abolish the sequence of the Sec7 domain (Supplementary Fig. S2C). Intracellular agglomerations of PIN1 were not observed in the *ben3-CRISPR* mutant similarly to other *big2* alleles confirming that loss of BEN3/BIG2 function results in the PIN1 localization defects. In addition, *BEN3::BEN3-GFP* construct (Supplementary Fig. S3A) rescued the BFA-response defect of the *big2* mutant line (SALK_024601), as judged by clear intracellular PIN1 accumulation as seen in wildtype root (Fig. 1 A, B). Taken together, these results demonstrate that *BEN3* gene encodes BIG2 ARF GEF.

Fluorescent proteins fused to BEN3/BIG2 localize at the TGN/EE

To gain insight into the sites of *BEN3/BIG2* expression and protein localization, we characterized fluorescent signals in *BEN3::BEN3-GFP* plants. Fluorescence microscopy revealed that *BEN3::BEN3-GFP* was broadly expressed in tissues including root meristem (Supplementary Fig. S3B). Root epidermis was then inspected by confocal microscopy. Punctate green fluorescent signals were

detected in the *BEN3::BEN3-GFP* line and the BEN3-GFP positive structures were rapidly labeled with a lipophilic styryl dye FM4-64, which can be used as endocytic tracer in various cells including Arabidopsis root epidermal cells (Fig. 2 A). It has been shown that FM4-64, initially incorporated into the plasma membrane, is gradually transported to early endosome, late endosome and vacuolar membrane (Ueda et al., 2001; Jaillais et al., 2008). Therefore, we speculated that the BEN3 localizes to early endosomal compartments. To determine the identity of the endosomal compartments labeled with BEN3-FP, we introduced *BEN3-RFP* into wildtype Col-0 line and confirmed that both BEN3-RFP and BEN3-GFP exhibited punctate fluorescent signals, which colocalized in root epidermal cells when co-expressed (Fig. 2 B). Fluorescent protein fused to various endosomal proteins were then co-expressed with BEN3-RFP. SNARE protein SYP61-, ARF GEF BEN1/MIN7-, and Sec1-Munc18 protein BEN2/VPS45- fused FPs predominantly localize at the TGN/EE (Robert et al. 2008; Tanaka et al. 2009; Tanaka et al. 2013). ARF1A1C/BEX1-GFP localize at the TGN/EE and Golgi apparatus (Xu and Scheres, 2005; Tanaka et al., 2014). Signals from these markers clearly overlapped with that of BEN3-RFP, indicating that BEN3-RFP localize at TGN/EE (Fig. 2 B). In contrast, fluorescent proteins fused to Rab GTPase ARA7, ARF GEF GNOM and GNOM-LIKE1 (GNL1), which mainly localize at the prevacuolar compartment / multi-vesicular body (PVC/MVB) and Golgi apparatus (Ueda et al., 2001; Geldner et al., 2003; Richter et al., 2007; Teh and Moore, 2007; Naramoto et al., 2014b) exhibited only marginal overlap with BEN3-RFP (Fig. 2 C, D). Consistent with BFA sensitive alteration in subcellular location of TGN/EE, treatment of Arabidopsis seedlings with BFA caused rapid agglomeration of BEN3-GFP signals (Supplementary Fig. S3C). Altogether, these results indicated that BEN3-FP localize predominantly to the TGN/EE.

BEN3/BIG2 is involved in PIN1 trafficking from TGN/EE to the PM

Reduced BFA sensitivity of PIN1 localization in the *ben3* mutants and BEN3/BIG2 localization at the TGN/EE suggest its role in PIN trafficking at the TGN/EE. We speculated that BEN3/BIG2 might be involved in trafficking from TGN/EE to the PM or other destination. To visualize trafficking of newly synthesized PIN1 protein, we used Arabidopsis line harboring an estradiol-inducible PIN1 construct (XVE-PIN1)(Petrášek et al., 2006). Transcription of *PIN1* was induced by temporally adding β-Estradiol and seedling roots were incubated in normal 1/2 MS medium to allow protein synthesis and trafficking (Supplementary Fig. S4A). In the wildtype seedlings harboring XVE-PIN1, ectopically induced PIN1 proteins in root epidermal cells did not reach the PM within 3 hours after the estradiol treatment, although PIN1 proteins were detectable as intracellular signals (Supplementary Fig. S4B). Under our experimental condition, PM-localized PIN1 was reproducibly detected in root epidermal cells 5 hours after the estradiol treatment (Supplementary Fig. S4B). As judged by the appearance of the immuno-stained anti-PIN1 signals in root epidermal cells, incubation with estradiol for 5 or 30 minutes appeared to result in comparable amount of new PIN1 protein synthesis (Supplementary Fig. S4B). To compare trafficking of estradiol-induced PIN1 proteins in wildtype and mutants, XVE-PIN1 was introduced into *ben1-1* and *ben3-1* background. In both genetic backgrounds, induced PIN1 was detectable at the PM within 5 hours after estradiol induction (Fig. 3 A, B). To evaluate the effect of BFA on the delivery of newly synthesized PIN1, BFA was added 2 hours after the estradiol treatment and kept for 3 hours. In XVE-PIN1 control line, BFA clearly induced agglomeration of intracellular PIN1 signals and strongly reduced the PM PIN1 localization. However, in the *ben3-1* background, clear PM PIN1 signals were detectable even in the presence of BFA (Fig. 3 C, D). In the *ben1-1* mutant background, induced PIN1 proteins were often detected from the PM and intracellular compartments

under the same condition (Fig. 3 C, D). These results show that trafficking of PIN1 from TGN/EE to the PM is inhibited by BFA and its sensitivity to BFA is affected by *ben1* and *ben3* mutations.

BFA-sensitive BEN1/MIN7 localization at the BFA compartment requires BEN3/BIG2

Both BEN1/MIN7 and BEN3/BIG2 ARF GEFs localize to the TGN/EE and are required for BFA-sensitive PIN1 trafficking (Figs. 2, 3). These findings prompted us to examine whether there is any mutual regulation between these two ARF GEF components. In the presence of BFA, BEN1/MIN7 localizes to the BFA compartment in wildtype root epidermal cells (Tanaka et al. 2009; Fig. 4 A; Supplementary Fig. S5). However, this BFA-dependent agglomeration of BEN1/MIN7 was suppressed in the *ben3* mutant background. This phenotype was recovered by *BEN3::BEN3-GFP* (Supplementary Fig. S5), suggesting that the mutations in BEN3/BIG2 is responsible for the altered distribution of BEN1-positive endosomes.

BEN3-RFP rapidly agglomerated following BFA treatment in wildtype background in various cell types including root epidermis, cortex and stele (Fig. 4 B). To test if the BFA-dependent BEN3-RFP distribution depends on BEN1, we introduced BEN3-RFP into *ben1-1* mutant background. As in wildtype background, rapid agglomeration of BEN3-RFP was detectable 10 minutes after the onset of BFA treatment in *ben1-1* mutant background (Fig. 4 B), revealing no or only minor impact of the *ben1* mutation in terms of BFA-sensitive BEN3-RFP localization. These results show that BFA-sensitive localization of BEN1/MIN7 depends on the BEN3/BIG2 activity but not vice versa.

BEN3/BIG2 is involved in BFA-sensitive seedling growth

Our results suggest that BEN3/BIG2 is involved in BFA sensitive trafficking at the TGN/EE in seedling root. However, *ben3* single mutants did not show any discernible defect in seedling growth (Fig. 5). In recent studies, it has been suggested that BIG family ARF GEFs including BIG2 are jointly involved in shoot development (Richter et al., 2014) and apical hook maintenance (Jonsson et al., 2017). Among the BIG family members closely related to BEN3/BIG2 (e.g. BIG1, BIG3, BIG4), only BIG3 is resistant to BFA, whereas other two members are BFA sensitive (Geldner et al., 2003; Richter et al., 2014). Therefore, *ben3-1; big3* double mutant was generated and grown in the presence of various concentrations of BFA. As reported previously, growth of *big3* single mutant was hypersensitive to BFA and root growth of the *big3* mutant was almost completely inhibited in the presence of 2.5 μM BFA. However, in the presence of lower concentration of BFA (0.5 μM), growth of *big3* root was only moderately inhibited (Fig. 5). In contrast, root growth of *ben3-1; big3* double mutants was inhibited strongly at lower concentration of BFA (0.25 μM), indicating that BFA hypersensitive root growth phenotype of *big3* mutant was exaggerated by *ben3-1* mutation (Fig. 5). These results suggest that, together with BIG3 and other BFA sensitive ARF GEFs, BEN3/BIG2 positively regulates root growth.

Discussion

PIN1 auxin efflux protein is rapidly shuttling between the PM and endosomes (Geldner et al., 2001; Dhonukshe et al., 2007). Previously, we identified Arabidopsis mutant *ben3*, which exhibited an altered PIN1-GFP trafficking in response to BFA (Tanaka et al., 2009). In this work, we show that a mutation in a member of BIG family ARF GEF trafficking regulators, BIG2, is responsible for the *ben3* mutant phenotypes. We have particularly addressed the roles of BEN3/BIG2 in BFA-sensitive PIN1 trafficking and localization of another ARF GEF BEN1/MIN7 at TGN/EE.

BEN3/BIG2 is involved in BFA-induced PIN1 relocation

BIG family ARF GEFs share highly conserved domains called DCB, HUS, Sec7, HDS1, HDS2 and HDS3 (Mouratou et al., 2005). The *ben3-1* mutation was predicted to generate a premature stop codon at the 1580th codon, and result in partial truncation of C-terminal region. We isolated multiple *big2* mutant alleles (Supplementary Fig. S2) and all of them exhibited similar PIN1 relocation defects as visualized by BFA treatment (Fig. 1), suggesting that BEN3/BIG2 function was abolished in all the *ben3* and *big2* mutant alleles tested, including the *ben3-1* (Q1580*). Sequence analysis of the BEN3/BIG2 homologues from various plant species revealed that part of the C-terminal region was moderately conserved among the BIG2 homologues (Supplementary Fig. S1B). RT-PCR experiment suggested that at least partial BEN3/BIG2 transcripts were generated in the *ben3-1* mutant. Thus our results shed light on a potentially important role of the C-terminal domain of BEN3/BIG2, although this region is not highly conserved in other members of Arabidopsis BIG family proteins. It remains to be determined whether the *ben3-1* mutation affected turnover, localization or functionality of the BIG2 ARF GEF. In

any case, the common phenotypes of all tested *ben3* alleles along with the complementation by BEN3-FP fusion proteins demonstrate that loss of BEN3/BIG2 function results in reduced intracellular accumulation of PIN1 in response to BFA.

BEN3/BIG2 is involved in trafficking of PIN1 to the plasma membrane

In plant cells, newly synthesized and endocytosed PM proteins are targeted to TGN/EE and transported to the PM or to the vacuole for degradation (Viotti et al., 2010; Uemura, 2016). In Arabidopsis, BFA alters organization of endosomes and inhibits exocytosis of PM proteins including PIN1, causing rapid accumulation of endocytosed and newly synthesized PM proteins in BFA compartments (Geldner et al., 2001; Dettmer et al., 2006; Richter et al., 2014; Jasik et al. 2016). Besides endocytic recycling and secretion of newly synthesized proteins to the PM, vacuolar targeting is also inhibited by BFA (Kleine-Vehn et al., 2008b). Similarly, genetic inhibition of ARF1 interferes with trafficking of PM and vacuolar proteins (Lee et al., 2002; Takeuchi et al., 2002; Pimpl et al., 2003; Kleine-Vehn et al., 2008b; Tanaka et al., 2014).

In this work, we showed that BFA-induced accumulation of PIN1 at the BFA compartment requires BEN3/BIG2 ARF GEF. These results suggest that BEN3/BIG2 is involved in transport of PIN1 to the PM, to the vacuole, or both. To gain insight into the trafficking pathway involving BEN3/BIG2, we used conditional expression of PIN1 to evaluate PIN1 trafficking to the PM. Under our experimental condition, BFA induced PIN1 accumulation at the BFA compartment and inhibited PIN1 delivery to the PM (Fig. 3). This BFA effect on the PM targeting was diminished in the *ben3* mutant background, suggesting that BEN3 is involved in endosome to PM trafficking. We speculate that exocytosis-related membranes might be intracellularly sequestered in BEN3-dependent manner in the presence of BFA (Supplementary Fig. S7). In the absence of BEN3, the sequestrating mechanism would be relieved and

BFA-resistant ARF GEF might efficiently deliver PIN1 protein to the PM (Supplementary Fig. S7). Richter et al. (2014) demonstrated that BIG3 ARF GEF is resistant to BFA and is required for trafficking of newly synthesized PIN1-RFP to the PM. Opposite phenotypes of *ben3* and *big3* suits very well with the BFA-resistant nature of BIG3 and sequence-based prediction of BEN3/BIG2 as being BFA sensitive (Geldner et al., 2003). In the *ben3* mutant, relative contribution of BFA-resistant ARF GEF BIG3 at the TGN/EE might be increased and this might account for the reduced PIN1 agglomeration phenotype of *ben3* (Supplementary Fig. S7). In support of this, comparing with *ben3* single mutant, *ben3; big3* double mutants exhibited increased PIN1-GFP agglomeration in the BFA compartment (Supplementary Fig. S6).

It has been proposed that BIG1 to BIG4 have redundant role in supporting plant development (Richter et al., 2014). Although *ben3* single mutants do not exhibit visible defect in seedling development, we showed that *ben3; big3* double mutants exhibit an enhanced BFA-hypersensitive root growth phenotypes (Fig. 5). Taken together, our results provide additional support for the redundant roles of BIG family ARF GEFs in plant development and TGN to PM trafficking in Arabidopsis.

BEN3/BIG2 is required for BFA-sensitive subcellular localization of BEN1/MIN7

Previously, we have identified Arabidopsis mutant *ben1*, which tend to accumulate less PIN1 in BFA compartment. BEN1/MIN7 localizes to the TGN/EE and accumulates at the core of BFA compartment following BFA treatment (Tanaka et al., 2009). Molecular cloning of *BEN3* enabled us to examine the possibility of mutual regulation between BEN1/MIN7 and BEN3/BIG2. Similar to the BEN1/MIN7, BEN3 localized to the TGN/EE (Fig.2) and BFA treatment induced rapid intracellular agglomeration of BEN3-GFP (Supplementary Fig. S3). This relocation seems to take place in a manner independent of

BEN1/MIN7 (Fig. 4, Supplementary Fig. S5). In contrast, our results show that localization of BEN1/MIN7 to the BFA compartment requires BEN3/BIG2 (Fig. 4, Supplementary Fig. S5). Thus, BFA-sensitive localization of BEN1/MIN7 and BEN3/BIG2 seem to involve distinct molecular mechanisms. Currently, our understanding of the mechanisms that recruit plant ARF GEFs to TGN/EE is very limited. It is noteworthy that an ARF-dependent mechanisms to recruit ARF GEFs to TGN in yeast and animals have been reported recently (Richardson et al., 2012; Lowery et al., 2013). In animal, a cascade model involving early and late ARF GEFs has been proposed: early ARF GEF GBF1, which localizes to pre-Golgi, Golgi apparatus and TGN, promotes localization of late ARF GEFs BIG1 and BIG2 to TGN to regulate vesicle coating. To better understand the ARF-dependent regulation of post-Golgi trafficking in plants, it would be important to reveal the interplay between different ARF GEFs and ARFs, as well as their impact on the downstream coating events.

Conclusion

Recent studies have revealed that multiple molecular components involved in PIN1 trafficking localize to the TGN/EE. A Sec1/Munc18 family protein BEN2/VPS45 is potentially involved in membrane fusion at the TGN/EE (Tanaka et al., 2013), whereas BEN1/MIN7 and BIG3 ARF GEFs, BEX1/ARF1A1C, BEX5/RabA1b, and a putative TRS120 VAN4 appear to regulate PIN1 exocytosis (Tanaka et al., 2009; Feraru et al., 2012; Naramoto et al., 2014a; Tanaka et al., 2014; Richter et al., 2014). In this work, we identified an additional ARF GEF component BEN3/BIG2 that regulates subcellular trafficking at the TGN/EE. BEN3 localization and trafficking defects of *ben3* strongly suggest that BEN3/BIG2 is involved in TGN/EE to PM trafficking. Moreover, our analysis using the trafficking inhibitor BFA suggested that different members of BIG class ARF GEFs could play distinct molecular functions and/or drug sensitivity at the TGN/EE. Although the highly redundant nature of some of the trafficking machinery is

a major obstacle to functional analyses, recently emerged information on the trafficking components, together with pharmacological tools including very recently identified novel trafficking inhibitors (Robert et al., 2008; Drakakaki et al., 2011; Doyle et al., 2015; Li et al., 2017) would facilitate our understanding of the intracellular trafficking through TGN/EE in plants.

Materials and Methods

Plant materials

Following Arabidopsis lines have been described previously: *pPIN1::PIN1-GFP* (Benkova et al. 2003); XVE-PIN1 (Petrášek et al., 2006; Mravec et al., 2008), *ben1-1; pPIN1::PIN1-GFP* (Tanaka et al. 2009); *ben3-1; pPIN1::PIN1-GFP* (Tanaka et al. 2009); *P35S::BEN1-GFP* (Tanaka et al. 2014). *ben3-1; P35S::BEN1-GFP*, *ben1-1; BEN3-TagRFP*, *big3* (SALK_044617)*; pPIN1::PIN1-GFP*, and *ben3-1; big3; pPIN1::PIN1-GFP* lines were generated by genetic crossing. *BEN3::BEN3-TagRFP* and *BEN3::BEN3-mTagGFP* lines were generated by transforming wildtype (Col-0), *ben3-1; PIN1-GFP*, or SALK_024601 (*ben3-2*) mutants using the floral dip method (Clough and Bent, 1998) essentially as described and basta- or hygromycin resistant T_1 plants were selected.

For genotyping of *ben3-1* allele, part of the *BEN3/BIG2* gene was amplified by PCR using BEN3-5629F and BEN3-5855R_Pv primers. The PCR product was then digested with PvuII. T-DNA insertion mutants (SALK_093944; SALK_016558; SALK_024601) were obtained from the Nottingham Arabidopsis Stock Center and PCR genotyped using following primers. For *ben3-2* (SALK_024601) and *ben3-3* (SALK_016558): BEN3_4115F, BEN3_5197R, LBb1-7510; and for *ben3-944* (SALK_093944): BEN3_430F, BEN3_1557R, and LBb1-7510 (Table S2).

The CRISPR/Cas9-induced *ben3* mutant allele was generated by transforming wildtype Col-0 plants with the guide RNA construct (pHSE401-gR2-BEN3). Genomic DNA was isolated from hygromicin-resistant T_1 plants and PCR genotyped by restriction digestion using MluI. For PCR-genotyping of *ben3-CRISPR* allele, PCR was performed with following primers and PCR fragment was digested with MluI: BEN3_1985F, BEN3_ 2532R (Table S2).

Chemical treatment

Treatment with BFA (Invitrogen B7450) was performed at 25 µM or 50 µM, diluted from 50 mM DMSO stock in liquid 1/2 MS medium at 21°C for indicated duration. β-estradiol (Sigma E2750) was diluted from 1 mM DMSO stock in the liquid medium. For induction of XVE-PIN1, 4 day-old seedlings were incubated in the β-estradiol containing liquid medium for 5 or 30 minutes, washed with normal liquid medium and further incubated as indicated. For growing seedling on BFA-containing plates, approximately 20 seedlings from each genotype were sown on 1/2 MS media solidified with 0.4% phytagel containing DMSO (1:1000) or different concentration of BFA. After storing at 4℃ for 2-4 days, they were transferred to the growth chamber (21°C, continuous light).

Molecular cloning of BEN3, expression analysis, and DNA construction

The *ben3-1* mutant was backcrossed two times with the PIN1-GFP parental line, and putative homozygous line was established by fluorescence-based phenotypic evaluation in F_3 generation and subjected to deep sequencing essentially as described (Depuydt et al., 2013).

For RT-PCR, total RNA was extracted from 5 day-old seedlings by RNeasy plant mini kit (Qiagen), treated with DNaseI and subjected to first-strand synthesis using SuperScript III reverse transcriptase (Thermo Fisher Scientific) with oligo (dT) primer. Aliquots of the first-strand cDNA were used as templates for RT-PCR reactions using following primers: BEN3_1985F and BEN3_2532R (Set 1); BEN3_4115F and BEN3_5197R (Set 2); ACT7_F and ACT7_R. Details of the primers are listed in Table S2.

To generate BEN3-TagRFP construct, TagRFP-As (Evrogen) and *BEN3* 3' non-coding region were PCR amplified with primers TagRFP_F_As, TagRFP_R_Xm, B3_ter_Xm_F and B3_ter_R_N (Table S2), digested with BspI, XmaI and NotI and cloned into BspI and Not I sites of a pEX-K-based cloning vector. A 2 kb *BEN3* upstream sequence was PCR amplified with primers B3minus2000F and B3minus1R. BEN3 coding region was amplified with primers B3_1F_As and B3_5379R_As (Table S2) and placed in front of TagRFP-As by in-fusion reaction (Clontech) according to the manufacture's instruction to yield pEX-K-BEN3::BEN3-RFP. For generation of BEN3 promoter::BEN3-GFP construct, coding sequence for a green fluorescent protein with monomerizing A206K mutation mTagGFP (Subach et al., 2008) harboring adjacent AscI and XmaI sites was PCR synthesized, digested with AscI and XmaI, and replaced with TagRFP of the pEX-K-BEN3::BEN3-RFP. BEN3::BEN3-GFP and BEN3::BEN3-RFP fragments were linearized by BspI and NotI and cloned into NotI site of the binary vector pMLBarT or pHyg (Mitao-Shimizu, unpublished).

For guideRNA construct targeting BEN3, two guide RNA sequences (5'-GTTTTCTCAAAGACGCGTCAGGG-3' and 5'-CAAGGTGATGCATGCATATGTGG-3' were cloned into the pHSE401 vector essentially as described (Xing et al., 2014).

Immunostaining and microscopy

Whole mount immunostaining was performed as described (Sauer et al., 2006). Following antibodies were used: rabbit anti-PIN1 (1:1000 or 1:2000; Paciorek et al. 2005), rabbit anti-MIN7 (1:1000)(Nomura et al., 2006), rabbit anti-SEC21 (1:1000; Agrisera AS08 327), rabbit anti-BiP (1:1000; Agrisera AS09 481) primary antibodies and Cy3-conjugated secondary anti-rabbit (1:600; Sigma C2306) antibody.

After the immuno-staining procedure, specimens were mounted on slides with PBS-glycerol containing an anti-fading reagent (25 mg/mL 1,4-Diazabicyclo-octane) or ClearSee solution (Kurihara et al., 2015). To observe PIN1-GFP, BEN1-GFP and BEN3-RFP in chemical-treated roots, seedlings were fixed in PFA solution [4% paraformaldehyde, phosphate-buffered saline (1xPBS), 0.05% Triton X-100] for 1h under vacuum, washed with 1xPBS for 30-60 min., and cleared in the ClearSee solution. Confocal laser scanning microscopy was performed by Carl Zeiss LSM710 microscope with 40x dry lens (Carl Zeiss, N/A 0.95) or 63x oil immersion lens (Carl Zeiss, N/A 1.40). Optical sectioning microscopy was done by Keyence BZX700 microscope with 40x water immersion lens (NIKON CFI60 N/A 1.25).

Quantification of intracellular accumulation of PIN1 and colocalization

For quantification of agglomerated anti-PIN1 immunofluorescence signals, stele cells within 150-200 µm above the quiescent center were selected for analysis. Intracellular PIN1 signals whose cross section area larger than 0.5 µm2 was counted as agglomeration. Frequency of agglomeration per cell was determined in at least 60 cells from each genotype and was subjected for statistic analysis (Mann-Whitney, two-tailed, non-parametric test) using PRISM software (GraphPad Software, Inc.).
To evaluate colocalization of subcellular markers, images from at least 5 seedlings were scanned with the simultaneous scanning mode using 63x oil immersion lens. Signals above background were selected and colocalization coefficient was calculated with ZEN 2009 software (Carl Zeiss).

Funding

This work has been partly supported by JSPS KAKENHI (23012026 and 16H04806 to HT). Part of the work was realized in CEITEC – Central European Institute of Technology (CZ.1.05/1.1.00/02.0068). The research leading to these results has received funding from the Czech Science Foundation GAČR

(GA13-40637S) to JF.

Acknowledgments

We thank Ben Scheres, Gerd Jürgens, Glenn R. Hicks, Ian Moore, Kinya Nomura, Natasha Raikhel, Niko Geldner and Qi-Jun Chen, Sheng Yang He for kindly providing published material; Matouš Glanc for technical advice, Yasushi Shiimzu-Mitao for providing a binary vector and Kayoko Kawamura for technical assistance.

References

Adamowski, M. and Friml, J. (2015) PIN-Dependent Auxin Transport: Action, Regulation, and Evolution. Plant Cell 27: 20–32.

Benková, E., Michniewicz, M., Sauer, M., Teichmann, T., Seifertová, D., Jürgens, G., et al. (2003) Local, Efflux-Dependent Auxin Gradients as a Common Module for Plant Organ Formation. Cell 115: 591–602.

Clough, S.J. and Bent, A.F. (1998) Floral dip: A simplified method for Agrobacterium-mediated transformation of Arabidopsis thaliana. Plant J. 16: 735–743.

Depuydt, S., Rodriguez-Villalon, A., Santuari, L., Wyser-Rmili, C., Ragni, L., Hardtke, C.S. (2013) Suppression of *Arabidopsis* protophloem differentiation and root meristem growth by CLE45 requires the receptor-like kinase BAM3. Proc. Natl. Acad. Sci. USA 110: 7074-7079.

Dettmer, J., Hong-Hermesdorf, A., Stierhof, Y.-D., and Schumacher, K. (2006) Vacuolar H+-ATPase Activity Is Required for Endocytic and Secretory Trafficking in Arabidopsis. Plant Cell 18: 715–730.

Dhonukshe, P., Aniento, F., Hwang, I., Robinson, D.G., Mravec, J., Stierhof, Y.D., et al. (2007) Clathrin-Mediated Constitutive Endocytosis of PIN Auxin Efflux Carriers in Arabidopsis. Curr. Biol. 17: 520–527.

Ding, Z., Galván-Ampudia, C.S., Demarsy, E., Łangowski, Ł., Kleine-Vehn, J., Fan, Y., et al. (2011) Light-mediated polarization of the PIN3 auxin transporter for the phototropic response in Arabidopsis. Nat. Cell Biol. 13: 447–52.

Doyle, S.M., Haeger, A., Vain, T., Rigal, A., Viotti, C., Łangowska, M., et al. (2015) An early secretory pathway mediated by GNOM-LIKE 1 and GNOM is essential for basal polarity establishment in Arabidopsis thaliana. Proc. Natl. Acad. Sci. USA 112: E806-E815.

Drakakaki, G., Robert, S., Szatmari, A.-M., Brown, M.Q., Nagawa, S., Van Damme, D., et al. (2011) Clusters of bioactive compounds target dynamic endomembrane networks in vivo. Proc. Natl. Acad. Sci. USA 108: 17850–17855.

Drdová, E.J., Synek, L., Pečenková, T., Hála, M., Kulich, I., Fowler, J.E., et al. (2013) The exocyst complex contributes to PIN auxin efflux carrier recycling and polar auxin transport in Arabidopsis. Plant J. 73: 709–719.

Du, Y., Tejos, R., Beck, M., Himschoot, E., Li, H., Robatzek, S., et al. (2013) Salicylic acid interferes with clathrin-mediated endocytic protein trafficking. Proc. Natl. Acad. Sci. USA 110: 7946–7951.

Feraru, E., Feraru, M.I., Asaoka, R., Paciorek, T., De Rycke, R., Tanaka, H., et al. (2012) BEX5/RabA1b Regulates trans-Golgi Network-to-Plasma Membrane Protein Trafficking in Arabidopsis. Plant Cell 24: 3074–3086.

Friml, J., Benková, E., Blilou, I., Wiśniewska, J., Hamann, T., Ljung, K., et al. (2002a) AtPIN4 mediates sink-driven auxin gradients and root patterning in Arabidopsis. Cell 108: 661–673.

Friml, J., Vieten, A., Sauer, M., Weijers, D., Schwarz, H., Hamann, T., et al. (2003) Efflux-dependent auxin gradients establish the apical-basal axis of Arabidopsis. Nature 426: 147–153.

Friml, J., Wiśniewska, J., Benková, E., Mendgen, K., and Palme, K. (2002b) Lateral relocation of auxin efflux regulator PIN3 mediates tropism in Arabidopsis. Nature 415: 806–809.

Gälweiler, L., Guan, C., Müller, A., Wisman, E., Mendgen, K., Yephremov, A., et al. (1998) Regulation of Polar Auxin Transport by AtPIN1 in *Arabidopsis* Vascular Tissue. Science 282: 2226–2230.

Geldner, N., Anders, N., Wolters, H., Keicher, J., Kornberger, W., Muller, P., et al. (2003) The Arabidopsis GNOM ARF-GEF mediates endosomal recycling, auxin transport, and auxin-dependent plant growth. Cell 112: 219–230.

Geldner, N., Friml, J., Stierhof, Y.D., Jürgens, G., and Palme, K. (2001) Auxin transport inhibitors block

PIN1 cycling and vesicle trafficking. Nature 413: 425–428.

Goodstein, D.M., Shu, S., Howson, R., Neupane, R., Hayes, R.D., Fazo, J., et al. (2012) Phytozome: A comparative platform for green plant genomics. Nucleic Acids Res. 40: D1178-D1186.

Hazak, O., Bloch, D., Poraty, L., Sternberg, H., Zhang, J., Friml, J., et al. (2010) A Rho scaffold integrates the secretory system with feedback mechanisms in regulation of auxin distribution. PLoS Biol. 8: e1000282.

Jaillais, Y., Fobis-Loisy, I., Miège, C., and Gaude, T. (2008) Evidence for a sorting endosome in Arabidopsis root cells. Plant J. 53: 237–247.

Jásik, J., Bokor, B., Stuchlík, S., Mičieta, K., Turňa, J., and Schmelzer, E. (2016) Effects of auxins on PIN-FORMED2 (PIN2) dynamics are not mediated by inhibiting PIN2 endocytosis. Plant Physiol. 172: 1019–1031.

Jonsson, K., Singh, R.K., Gendre, D., and Bhalerao, R.P. (2017) Ethylene Regulates Differential Growth via BIG ARF-GEF-Dependent Post-Golgi Secretory Trafficking in Arabidopsis. 29: 1039–1052.

Kitakura, S., Vanneste, S., Robert, S., Löfke, C., Teichmann, T., Tanaka, H., et al. (2011) Clathrin mediates endocytosis and polar distribution of PIN auxin transporters in Arabidopsis. Plant Cell 23: 1920–1931.

Kleine-Vehn, J., Dhonukshe, P., Sauer, M., Brewer, P.B., Wiśniewska, J., Paciorek, T., et al. (2008a) ARF GEF-Dependent Transcytosis and Polar Delivery of PIN Auxin Carriers in Arabidopsis. Curr. Biol. 18: 526–531.

Kleine-Vehn, J., Leitner, J., Zwiewka, M., Sauer, M., Abas, L., Luschnig, C., et al. (2008b) Differential degradation of PIN2 auxin efflux carrier by retromer-dependent vacuolar targeting. Proc. Natl. Acad. Sci. USA 105: 17812–17817.

Kurihara, D., Mizuta, Y., Sato, Y., and Higashiyama, T. (2015) ClearSee: a rapid optical clearing reagent for whole-plant fluorescence imaging. Development 142: 4168–4179.

Lee, M.H., Min, M.K., Lee, Y.J., Jin, J.B., Shin, D.H., Kim, D.H., et al. (2002) ADP-Ribosylation Factor 1 of Arabidopsis Plays a Critical Role in Intracellular Trafficking and Maintenance of Endoplasmic Reticulum Morphology in Arabidopsis. Plant Physiol. 129: 1507–1520.

Leitner, J., Petrášek, J., Tomanov, K., Retzer, K., Parezova, M., Korbei, B., et al. (2012) Lysine63-linked ubiquitylation of PIN2 auxin carrier protein governs hormonally controlled adaptation of Arabidopsis root growth. Proc. Natl. Acad. Sci. 109: 8322–8327.

Li, R., Rodriguez Furlan, C., Wang, J., van de Ven, W., Gao, T., Raikhel, N. V, et al. (2017) Different Endomembrane Trafficking Pathways Establish Apical and Basal Polarities. Plant Cell 29: 90-108.

Löfke, C., Zwiewka, M., Heilmann, I., Van Montagu, M.C.E., Teichmann, T., and Friml, J. (2013) Asymmetric gibberellin signaling regulates vacuolar trafficking of PIN auxin transporters during root gravitropism. Proc. Natl. Acad. Sci. USA 110: 3627–32.

Lowery, J., Szul, T., Styers, M., Holloway, Z., Oorschot, V., Klumperman, J., et al. (2013) The Sec7 guanine nucleotide exchange factor GBF1 regulates membrane recruitment of BIG1 and BIG2 guanine nucleotide exchange factors to the trans-Golgi network (TGN). J. Biol. Chem. 288: 11532–11545.

Marhavý, P., Bielach, A., Abas, L., Abuzeineh, A., Duclercq, J., Tanaka, H., et al. (2011) Cytokinin Modulates Endocytic Trafficking of PIN1 Auxin Efflux Carrier to Control Plant Organogenesis. Dev. Cell 21: 796–804.

Men, S., Boutté, Y., Ikeda, Y., Li, X., Palme, K., Stierhof, Y.-D., et al. (2008) Sterol-dependent endocytosis mediates post-cytokinetic acquisition of PIN2 auxin efflux carrier polarity. Nat. Cell

Biol. 10: 237–244.

Mouratou, B., Biou, V., Joubert, A., Cohen, J., Shields, D.J., Geldner, N., et al. (2005) The domain architecture of large guanine nucleotide exchange factors for the small GTP-binding protein Arf. BMC Genomics 6: 20.

Mravec, J., Petrášek, J., Li, N., Boeren, S., Karlova, R., Kitakura, S., et al. (2011) Cell plate restricted association of DRP1A and PIN proteins is required for cell polarity establishment in arabidopsis. Curr. Biol. 21: 1055–1060.

Mravec, J., Kubeš, M., Bielach, A., Gaykova, V., Petrášek, J., Skůpa, P., et al. (2008) Interaction of PIN and PGP transport mechanisms in auxin distribution-dependent development. Development 135: 3345–3354.

Müller, A., Guan, C., Gälweiler, L., Tänzler, P., Huijser, P., Marchant, A., et al. (1998) AtPIN2 defines a locus of AtPIN2 defines a locus of Arabidopsis for root gravitropism control. EMBO J. 17: 6903–6911.

Naramoto, S., Kleine-Vehn, J., Robert, S., Fujimoto, M., Dainobu, T., Paciorek, T., et al. (2010) ADP-ribosylation factor machinery mediates endocytosis in plant cells. Proc. Natl. Acad. Sci. USA 107: 21890–21895.

Naramoto, S., Nodzyński, T., Dainobu, T., Takatsuka, H., Okada, T., Friml, J., et al. (2014a) VAN4 encodes a putative TRS120 that is required for normal cell growth and vein development in arabidopsis. Plant Cell Physiol. 55: 750–763.

Naramoto, S., Otegui, M.S., Kutsuna, N., de Rycke, R., Dainobu, T., Karampelias, M., et al. (2014b) Insights into the localization and function of the membrane trafficking regulator GNOM ARF-GEF at the Golgi apparatus in Arabidopsis. Plant Cell 26: 3062–3076.

Nomura, K., Debroy, S., Lee, Y.H., Pumplin, N., Jones, J., and He, S.Y. (2006) A bacterial virulence

protein suppresses host innate immunity to cause plant disease. Science 313: 220–223.

Paciorek, T., Zažímalová, E., Ruthardt, N., Petrášek, J., Stierhof, Y.-D., Kleine-Vehn, J., et al. (2005) Auxin inhibits endocytosis and promotes its own efflux from cells. Nature 435: 1251–1256.

Petrášek, J., Mravec, J., Bouchard, R., Blakeslee, J.J., Abas, M., Seifertová, D., et al. (2006) PIN proteins perform a rate-limiting function in cellular auxin efflux. Science 312: 914–918.

Pfister, A., Barberon, M., Alassimone, J., Kalmbach, L., Lee, Y., Vermeer, J.E.M., et al. (2014) A receptor-like kinase mutant with absent endodermal diffusion barrier displays selective nutrient homeostasis defects. Elife 3: e03115.

Pimpl, P., Hanton, S.L.S., Taylor, J.P., Pinto-dasilva, L.L., Denecke, J., and Lamberti, L. (2003) The GTPase ARF1p controls the sequence-specific vacuolar sorting route to the lytic vacuole. Plant Cell 15: 1242–1256.

Rakusová, H., Abbas, M., Han, H., Song, S., Robert, H.S., and Friml, J. (2016) Termination of Shoot Gravitropic Responses by Auxin Feedback on PIN3 Polarity. Curr. Biol. 26: 3026–3032.

Rakusová, H., Gallego-Bartolomé, J., Vanstraelen, M., Robert, H.S., Alabadí, D., Blázquez, M.A., et al. (2011) Polarization of PIN3-dependent auxin transport for hypocotyl gravitropic response in Arabidopsis thaliana. Plant J. 67: 817–826.

Richardson, B.C., McDonold, C.M., and Fromme, C.J. (2012) The Sec7 Arf-GEF Is Recruited to the trans-Golgi Network by Positive Feedback. Dev. Cell 22: 799–810.

Richter, S., Geldner, N., Schrader, J., Wolters, H., Stierhof, Y.-D., Rios, G., et al. (2007) Functional diversification of closely related ARF-GEFs in protein secretion and recycling. Nature 448: 488–492.

Richter, S., Kientz, M., Brumm, S., Nielsen, M.E., Park, M., Gavidia, R., et al. (2014) Delivery of endocytosed proteins to the cell-division plane requires change of pathway from recycling to

secretion. Elife 3: e02131.

Robert, S., Chary, S.N., Drakakaki, G., Li, S., Yang, Z., Raikhel, N. V, et al. (2008) Endosidin1 defines a compartment involved in endocytosis of the brassinosteroid receptor BRI1 and the auxin transporters PIN2 and AUX1. Proc. Natl. Acad. Sci. USA 105: 8464–8469.

Sauer, M., Paciorek, T., Benková, E., and Friml, J. (2006) Immunocytochemical techniques for whole-mount in situ protein localization in plants. Nat. Protoc. 1: 98–103.

Subach, O.M., Gundorov, I.S., Yoshimura, M., Subach, F. V., Zhang, J., Grüenwald, D., et al. (2008) Conversion of Red Fluorescent Protein into a Bright Blue Probe. Chem. Biol. 15: 1116–1124.

Swarup, R., Friml, J., Marchant, A., Ljung, K., Sandberg, G., Palme, K., et al. (2001) Localization of the auxin permease AUX1 suggests two functionally distinct hormone transport pathways operate in the Arabidopsis root apex. Genes Dev. 15: 2648–2653.

Takano, J., Noguchi, K., Yasumori, M., Kobayashi, M., Gajdos, Z., Miwa, K., et al. (2002) Arabidopsis boron transporter for xylem loading. Nature 420: 337–340.

Takano, J., Tanaka, M., Toyoda, A., Miwa, K., Kasai, K., Fuji, K., et al. (2010) Polar localization and degradation of Arabidopsis boron transporters through distinct trafficking pathways. Proc. Natl. Acad. Sci. USA 107: 5220–5225.

Takeuchi, H. and Higashiyama, T. (2016) Tip-localized receptors control pollen tube growth and LURE sensing in Arabidopsis. Nature 531: 245–248.

Takeuchi, M., Ueda, T., Yahara, N., and Nakano, A. (2002) Arfl GTPase plays roles in the protein traffic between the endoplasmic reticulum and the Golgi apparatus in tobacco and Arabidopsis cultured cells. Plant J. 31: 499–515.

Tanaka, H., Kitakura, S., Rakusová, H., Uemura, T., Feraru, M.I., de Rycke, R., et al. (2013) Cell Polarity and Patterning by PIN Trafficking through Early Endosomal Compartments in Arabidopsis

thaliana. PLoS Genet. 9: e1003540.

Tanaka, H., Kitakura, S., De Rycke, R., De Groodt, R., and Friml, J. (2009) Fluorescence Imaging-Based Screen Identifies ARF GEF Component of Early Endosomal Trafficking. Curr. Biol. 19: 391–397.

Tanaka, H., Nodzynski, T., Kitakura, S., Feraru, M.I., Sasabe, M., Ishikawa, T., et al. (2014) BEX1/ARF1A1C is required for BFA-sensitive recycling of PIN auxin transporters and auxin-mediated development in arabidopsis. Plant Cell Physiol. 55: 737–749.

Teh, O.-K. and Moore, I. (2007) An ARF-GEF acting at the Golgi and in selective endocytosis in polarized plant cells. Nature 448: 493–496.

Ueda, T., Yamaguchi, M., Uchimiya, H., and Nakano, A. (2001) Ara6, a plant-unique novel type Rab GTPase, functions in the endocytic pathway of Arabidopsis thaliana. EMBO J. 20: 4730–4741.

Uemura, T. (2016) Physiological roles of plant post-golgi transport pathways in membrane trafficking. Plant Cell Physiol. 57: 2013–2019.

Viotti, C., Bubeck, J., Stierhof, Y.-D., Krebs, M., Langhans, M., van den Berg, W., et al. (2010) Endocytic and secretory traffic in Arabidopsis merge in the trans-Golgi network/early endosome, an independent and highly dynamic organelle. Plant Cell 22: 1344–1357.

Watanabe, M., Tanaka, H., Watanabe, D., Machida, C., and Machida, Y. (2004) The ACR4 receptor-like kinase is required for surface formation of epidermis-related tissues in Arabidopsis thaliana. Plant J. 39: 298–308.

Xing, H.-L., Dong, L., Wang, Z.-P., Zhang, H.-Y., Han, C.-Y., Liu, B., et al. (2014) A CRISPR/Cas9 toolkit for multiplex genome editing in plants. BMC Plant Biol. 14: 327.

Xu, J. and Scheres, B. (2005) Dissection of Arabidopsis ADP-RIBOSYLATION FACTOR 1 Function in Epidermal Cell Polarity. Plant Cell 17: 525–536.

Legends to Figures

Fig. 1 *ben3* and *big2* mutants exhibit PIN1 relocation defects.

(A) Anti-PIN1 immunostaining of wildtype, *ben3* and *big2* alleles. BFA treatment (50 µM, 1h) caused intracellular accumulation of PIN1 in wildtype root vasculature (arrowheads), whereas *ben3-1* and *big2* homozygous mutants (*SALK_016558, SALK_024601, SALK_093944, ben3-CRISPR*) had less pronounced intracellular PIN1 agglomeration. In the SALK_024601 homozygous seedling containing the *BEN3::BEN3-GFP* construct, BFA induced clear PIN1 agglomeration as in wildtype (arrowheads). Scale bar: 10 µm.

(B) Quantitative evaluation of intracellular PIN1 signals. Frequencies of the agglomerated PIN1 signals from wildtype, *big2* homozygous mutant (*SALK_024601*) and the mutant harboring *BEN3-GFP* transgene (*BEN3-GFP; SALK_024601*) were presented with standard deviation. The p values obtained from Mann-Whitney test were: Col-0 (WT) versus *SALK_024601*, p=0.0013; *SALK_024601* versus *BEN3-GFP; SALK_024601*, p=0.0019; Col-0 (WT) versus *BEN3-GFP; SALK_024601*, p=0.3582.

Fig. 2 Fluorescent proteins fused to BEN3 localize at the TGN/EE.

(A) Root epidermis of *BEN3::BEN3-GFP* seedling labeled with an endocytic tracer FM4-64 (2 µM, 6 min.).

(B) Colocalization analysis using BEN3-RFP and proteins associated with TGN/EE.

(C) Visualization of BEN3-RFP, ARA7-YFP, GNOM-GFP and GNL1-YFP.

(D) Quantitative evaluation of colocalization. Values of colocalization coefficient were calculated using at least five seedlings expressing BEN3-RFP and indicated markers.

Scale bars: 5 μm.

Fig. 3 *ben3* mutation affects BFA-sensitive trafficking of PIN1 to the plasma membrane.

(A, B) Wildtype (Col-0), XVE-PIN1 on wildtype, *ben1-1* and *ben3-1* background treated with β-estradiol (1 μM, 5 min.) and incubated in 1/2 MS media for 2 hours (A) or 5 hours (B) were immunostained with anti-PIN1 antibody (red) and stained with DAPI (blue). Arrows indicate PM localized PIN1 signals.

(C) Seedlings incubated for 2 hours in 1/2 MS media after the β-estradiol treatment (1 μM, 5 min.) and subsequently in BFA containing media (25 μM, 3h). Asterisks indicate intracellular accumulation of PIN1 signal in an epidermal cell of the XVE-PIN1 on wildtype background.

(D) Quantification of PIN1 localization in BFA-treated root epidermal cells. Estradiol-induced PIN1 predominantly localized at the BFA compartment in the wildtype background (22/22 cells). In *ben1-1* background, comparable level of PIN1 signals were often detected both at the PM and intracellular dots (orange, 24/36 cells), whereas stronger PM localization of PIN1 was frequently observed in the *ben3-1* mutant background (red, 14/29 cells).

Scale bars: 10 μm.

Fig. 4 BFA-induced agglomeration of BEN1-GFP requires *BEN3*.

(A) Root vasculature of *ben1-2* (upper panels) and *ben3-1* (lower panels) mutants expressing *P35S::BEN1-GFP*.

(B) Longitudinal views of root meristem of wildtype (upper panels) and *ben1-2* mutants (lower panels) expressing *BEN3::BEN3-RFP*.

Seedlings were treated with BFA (25 µM) for indicated period, fixed and mounted in ClearSee. Scale bars: 50 µm.

Fig. 5 *ben3; big3* double mutants exhibit BFA-hypersensitive seedling growth phenotypes.

(A) Gross morphology of wildtype, *ben3-1*, *big3*, and *ben3-1;big3* seedlings. Wildtype and mutant seedlings were vertically grown on solid media containing various concentration of BFA or DMSO as control. Scale bar: 1 cm.

(B) Quantification of root length. Four day-old seedlings were subjected for analysis. Error bars indicate standard deviation.

Supplementary Fig. S1 *ben3-1* has a mutation in *BEN3/BIG2*.

(A) Domain organization of the BEN3/BIG2. The boxed regions, DCB, HUS, Sec7 and HDS1, HDS2 and HDS3 indicate the highly conserved regions. Positions of the *ben3* mutations relative to the domain organization of BEN3/BIG2 were indicated.

(B) Predicted amino acid sequences of the C-terminal region of BEN3/BIG2 and closely related homologues from various plant species. Following sequences were retrieved from Phytozome

database (Goodstein et al., 2012) and aligned using CLASTAL omega algorism (http://www.ebi.ac.uk/ Tools/msa/clustalo/). *Oryza sativa*: LOC_Os03g14260_1; *Marchantia polymorpha*: Mapoly0030s0155.1; *Physcomitrella patens*: Pp3c7_14180V3_1; *Volvox carteri*: Vocar_0056s0013_2 and *Chlamydomonas reinhardtii*: Cre09_g390319_t1_1. Amino acids which were identical in all protein sequences or more than four proteins were highlighted in orange and yellow, respectively. Position of the *ben3-1* mutation was indicated with an arrow.

(C) Complementation of *ben3-1* mutant phenotype. PIN1-GFP (green) was detected in *PIN1-GFP* (WT), *ben3-1; PIN1-GFP*, and *ben3-1; PIN1-GFP* harboring *BEN3-RFP* construct (*BEN3-RFP* > *ben3-1*). In the *BEN3-RFP* > *ben3-1* line, RFP (magenta) and merged images were also indicated. Scale bar: 10 μm.

Supplementary Fig. S2 Sites of *big2* mutations and transcript accumulation.

(A) Relative positions of mutations in the *BEN3/BIG2* gene. Coding regions were indicated by orange boxes. Set 1 and Set 2 indicate the regions examined by RT-PCR. T-DNAs were not drawn in scale.

(B) Characterization of *BEN3/BIG2* transcript accumulation in the mutants by RT-PCR. Set 1 and Set 2 represent different primer sets to amplify parts of *BEN3/BIG2* cDNA.

(C) CRISPR/Cas9-induced *ben3* allele. Site of mutation relative to the guide RNA and PAM sequence is indicated. Sequence analysis revealed that the *ben3-CRISPR* allele contained an insertion of a single nucleotide at the putative cleavage site (arrowhead).

Supplementary Fig. S3 Expression and localization of fluorescent protein-fused BEN3 in Arabidopsis seedlings.

(A) Schematic diagram showing the structure of *BEN3::BEN3-GFP* and *BEN3::BEN3-RFP* constructs.

(B) Wide-field views of fluorescent signals in *BEN3::BEN3-GFP* and *BEN3::BEN3-RFP* lines. Comparing to negative control, GFP and RFP signals above background were detected broadly in seedling roots.

(C) Visualization of BEN3-GFP and antibody-based subcellular markers in DMSO- and BFA-treated root epidermal cells. BEN3-GFP signals and immunofluorescence signals were shown in green and red, respectively. Scale bar: 5 μm.

Supplementary Fig. S4 Time-dependent subcellular localization of estradiol-induced PIN1.

(A) Experimental scheme showing the treatment with β-Estradiol (red box) and normal liquid media (white box) as well as typical subcellular localization of induced PIN1 protein.

(B) Representative PIN1 localization in root meristem. Anti-PIN1 antibody staining reveals that induced PIN1 initially localized in intracellular region in root epidermis and reaches to the PM by 5 hours after the onset of estradiol treatment.
Scale bar: 20 μm.

Supplementary Fig. S5 Localization of BEN1/MIN7 protein in BFA-treated root epidermal cells. Wildtype, *ben3* and *big2* mutants were BFA-treated (25 μM, 1h) and immunostained with anti-MIN7 antibody to visualize localization of BEN1/MIN7 proteins. As control, no signal above background was

detected in *ben1-2* mutant. Scale bar: 50 μm.

Supplementary Fig. S6 *big3* mutation suppresses the PIN1-GFP agglomeration defect of *ben3*. Agglomerations of PIN1-GFP in the root stele cells were less pronounced in BFA-treated *ben3-1* mutants. In contrast, *big3* mutants exhibited clear intracellular accumulations of PIN1-GFP. Under the same condition, clear agglomeration of PIN1-GFP was observed in the *ben3-1; big3* double mutants. Scale bar: 10 μm.

Supplementary Fig. S7 Schematic models for BFA-sensitive exocytic PIN1 trafficking.
In wildtype, both BFA-sensitive (blue) and resistant (green) ARF GEFs are involved in PIN1 trafficking from TGN/EE to the PM. In BFA-treated wildtype cells, BFA inhibits the action of sensitive GEFs, and causes accumulation of PIN1 (orange) at the TGN/EE. In this situation, PIN1 proteins are sequestered at the TGN/EE in a manner dependent on BFA-sensitive ARF GEFs including BEN3/BIG2. In the *ben3* single mutant, no discernible defect in PIN1 localization was observed without BFA treatment. In BFA-treated *ben3* mutant cells, exocytic pathway might be highly dependent on a BFA-resistant ARF GEF (e.g. BIG3).

Table S1 List of potential nucleotide substitution causing missense or nonsense mutations.

Table S2 List of oligonucleotides used in this study.

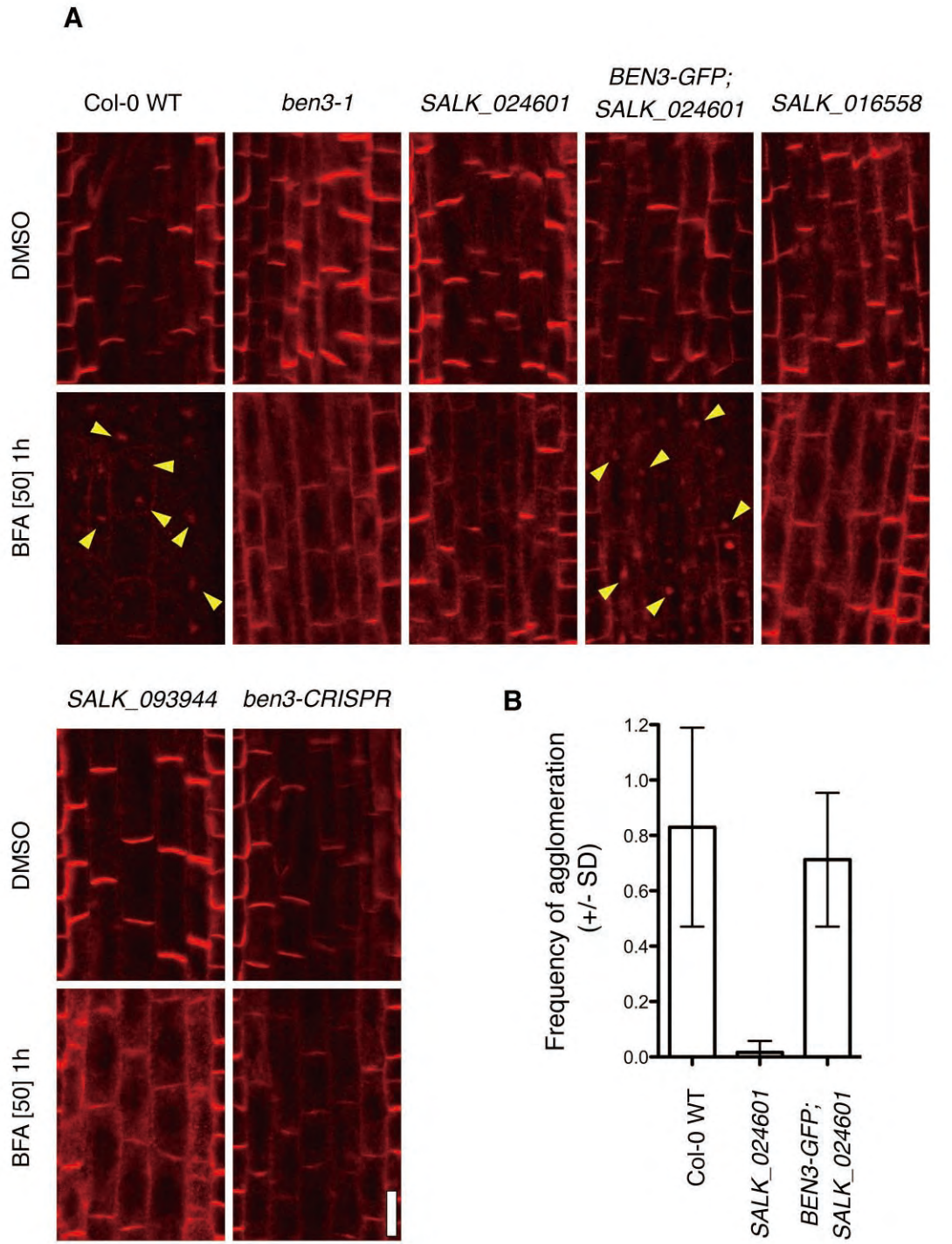
A
Col-0 WT
ben3-1
SALK_024601
BEN3-GFP;
SALK_024601
SALK_016558
DMSO
BFA [50] 1h
SALK_093944
ben3-CRISPR
DMSO
BFA [50] 1h
B
Frequency of agglomeration
(+/- SD)
1.2
1.0
0.8
0.6
0.4
0.2
0.0
Col-0 WT
SALK_024601
BEN3-GFP;
SALK_024601

Figure 1

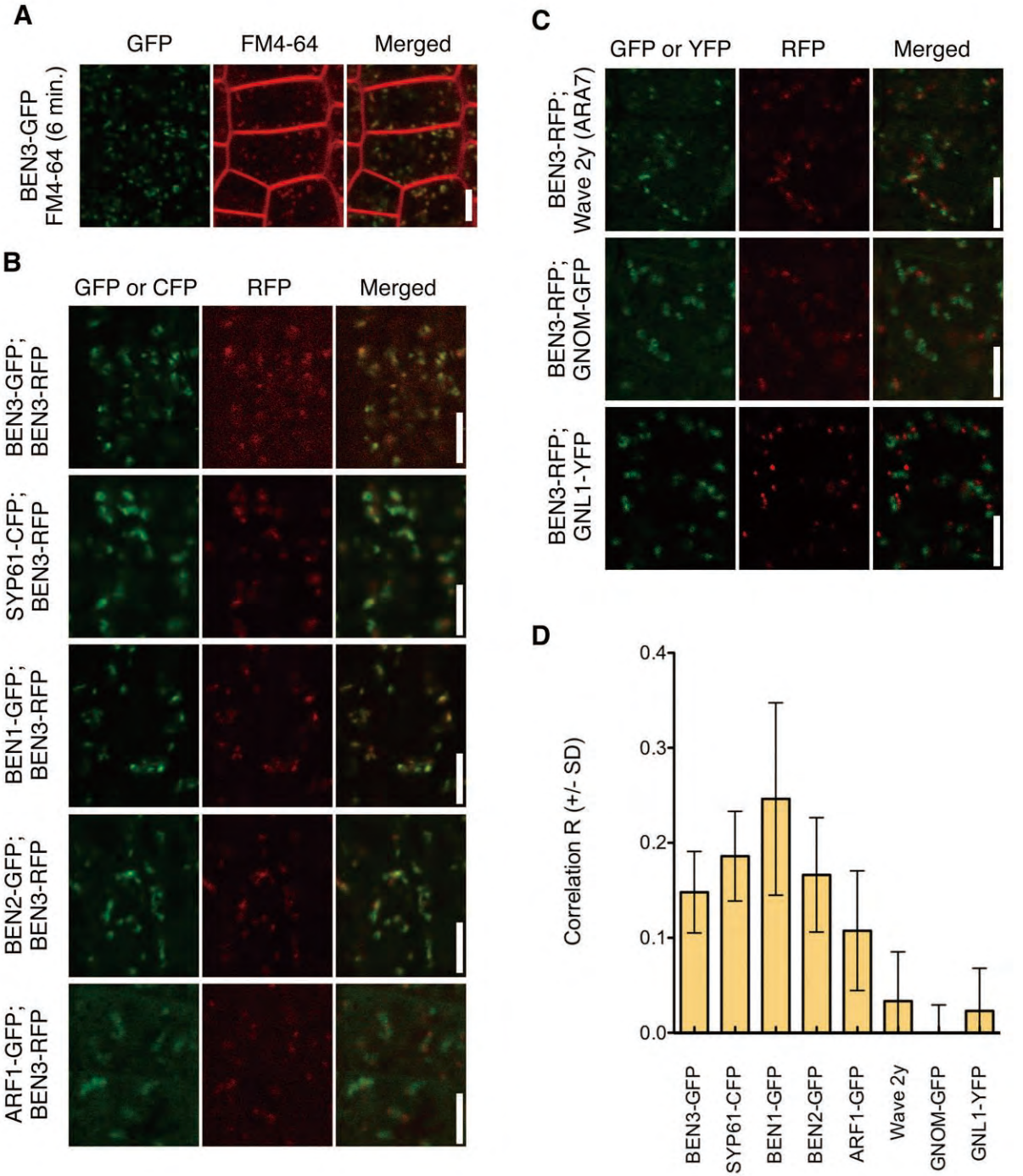
A
GFP
FM4-64
Merged
BEN3-GFP
FM4-64 (6 min.)
B
GFP or CFP
RFP
Merged
BEN3-GFP;
BEN3-RFP
SYP61-CFP;
BEN3-RFP
BEN1-GFP;
BEN3-RFP
BEN2-GFP;
BEN3-RFP
ARF1-GFP;
BEN3-RFP
C
GFP or YFP
RFP
Merged
BEN3-RFP;
Wave 2y (ARA7)
BEN3-RFP;
GNOM-GFP
BEN3-RFP;
GNL1-YFP
D
Correlation R (+/- SD)
0.4
0.3
0.2
0.1
0.0
BEN3-GFP
SYP61-CFP
BEN1-GFP
BEN2-GFP
ARF1-GFP
Wave 2y
GNOM-GFP
GNL1-YFP

Figure 2

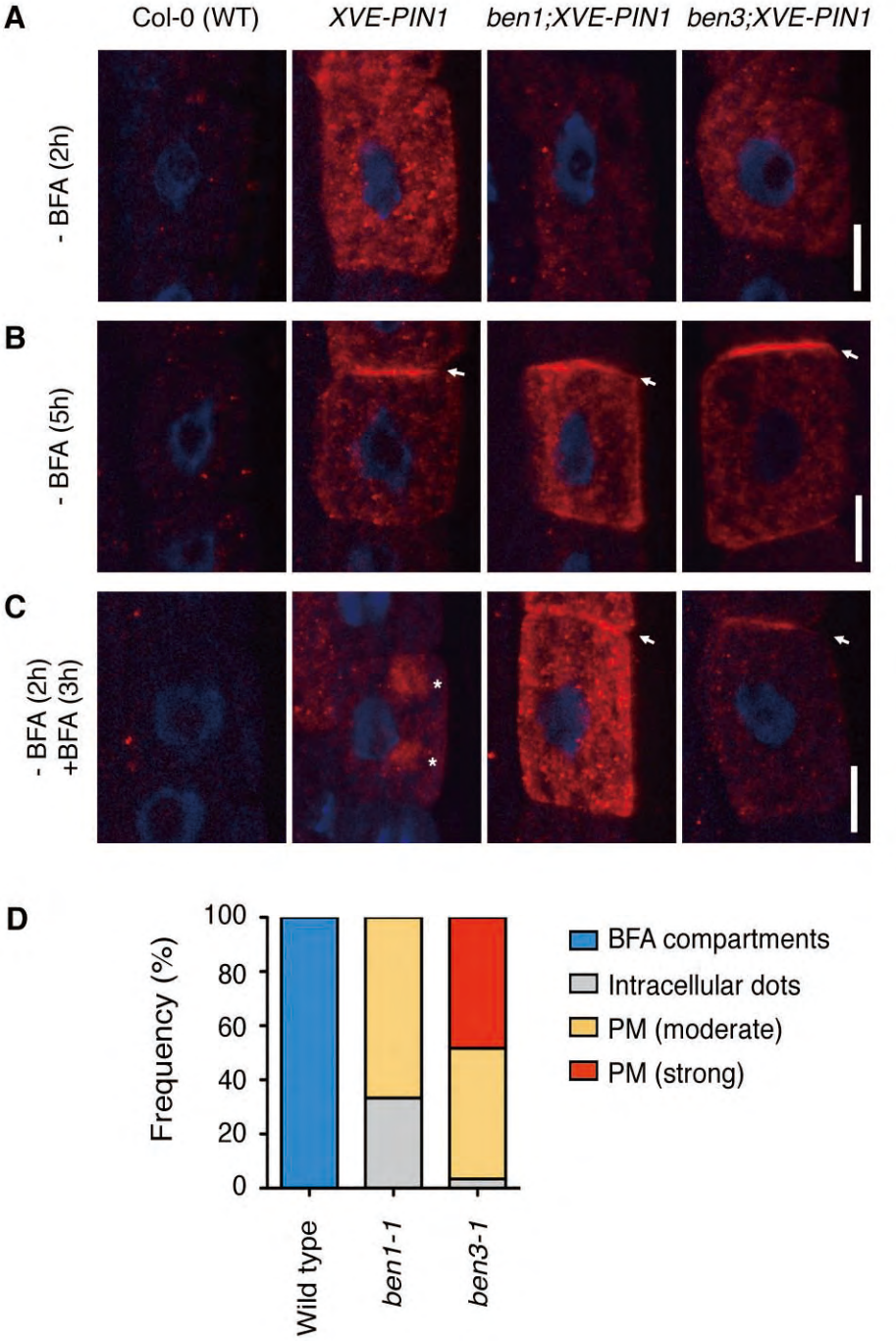
A
Col-0 (WT)
XVE-PIN1
ben1;XVE-PIN1
ben3;XVE-PIN1
- BFA (2h)
B
- BFA (5h)
C
- BFA (2h)
+BFA (3h)
*
*
D
Frequency (%)
100
80
60
40
20
0
Wild type
ben1-1
ben3-1
BFA compartments
Intracellular dots
PM (moderate)
PM (strong)

Figure 3

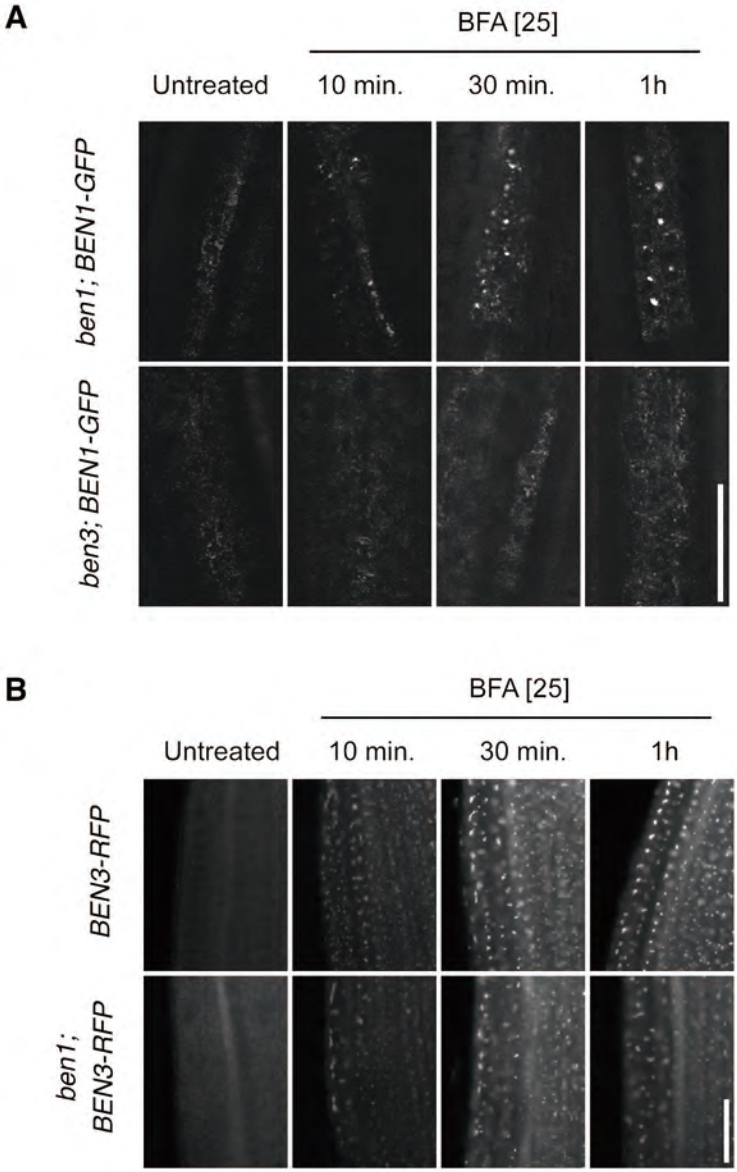
A
BFA [25]
Untreated
10 min.
30 min.
1h
ben1; BEN1-GFP
ben3; BEN1-GFP
B
BFA [25]
Untreated
10 min.
30 min.
1h
BEN3-RFP
ben1;
BEN3-RFP

Figure 4

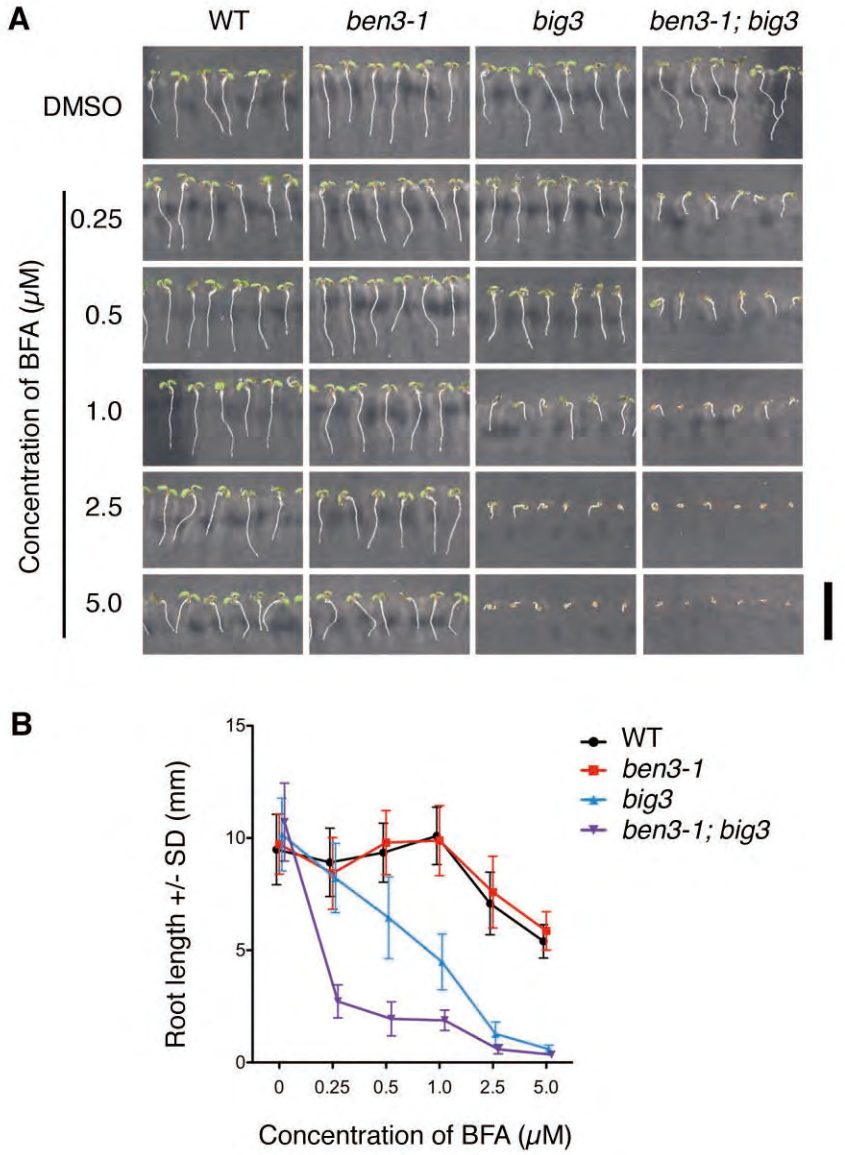
A
WT
ben3-1
big3
ben3-1; big3
DMSO
0.25
0.5
1.0
2.5
5.0
Concentration of BFA (μM)
B
Root length +/- SD (mm)
15
10
5
0
0
0.25
0.5
1.0
2.5
5.0
Concentration of BFA (μM)
WT
ben3-1
big3
ben3-1; big3

Figure 5